Field-flow fractionation of magnetic particles in a cyclic magnetic field

Yanping Bi, Xiaoxia Pan, Lei Chen, Qian-Hong Wan *

School of Pharmaceutical Science & Technology, Tianjin University, Tianjin 300072, China

ABSTRACT

Although magnetic field-flow fractionation (MgFFF) is emerging as a promising technique for characterizing magnetic particles, it still suffers from limitations such as low separation efficiency due to irreversible adsorption of magnetic particles on separation channel. Here we report a novel approach based on the use of a cyclic magnetic field to overcome the particle entrapment in MgFFF. This cyclic field is generated by rotating a magnet on the top of the spiral separation channel so that magnetic and opposing gravitational forces alternately act on the magnetic particles suspended in the fluid flow. As a result, the particles migrate transversely between the channel walls and their adsorption at internal channel surface is prevented due to short residence time which is controlled by the rotation frequency. With recycling of the catch-release process, the particles follow saw-tooth-like downstream migration trajectories and exit the separation channel at velocities corresponding to their sedimentation coefficients. A retention model has been developed on the basis of the combined effects of magnetic, gravitational fields and hydrodynamic flow on particle migration. Two types of core–shell structured magnetic microspheres with diameters of 6.04- and 9.40-μm were synthesized and used as standard particles to test the proposed retention theory under varying conditions. The retention ratios of these two types of particles were measured as a function of magnet rotation frequency, the gap between the magnet and separation channel, carrier flow rate, and sample loading. The data obtained confirm that optimum separation of magnetic particles with improved separation efficiency can be achieved by tuning rotation frequency, magnetic field gradient, and carrier flow rate. In view of the widespread applications of magnetic microspheres in separation of biological molecules, virus, and cells, this new method might be extended to separate magnetically labeled proteins or organisms for multiplex analyte identification and purification.

© 2011 Elsevier B.V. All rights reserved.

1. Introduction

Field-flow fractionation (FFF) is a powerful technique for separating macromolecular, colloidal and micron-sized particles, and has become a method of choice for analysis of polymeric and biologic materials [1–3]. FFF utilizes the transverse motion of analytes induced by an applied external field and separates them on the basis of their differential distribution in the laminar flow with a parabolic velocity profile. In principle any type of field can be used as long as it is capable of inducing transverse mass transport of the sample components. This has given rise to multiple subtechniques within the FFF family [4]. While crossflow, sedimentation, and thermal FFF are all commercially available, magnetic, electric, and acoustic FFF are currently undergoing intensive development and have yet to be commercialized [5]. Magnetic FFF (MgFFF) has been recognized as a potentially useful tool for characterizing magnetic particles

since its first demonstration by Vickrey and Garcia-Ramirez in 1980 [6]. Despite tremendous efforts devoted to the development of this technique, little progress has been made over the last 3 decades [7,8]. A major difficulty in such a system has been irreversible adsorption of magnetic analytes on flow channel walls causing excessive band broadening and accelerated deterioration of separation performance. To alleviate this problem, approaches based on mechanical vibration to the column [9], periodical intermittent magnetic field [10], increasing shear forces exerted on the analytes [11], and differential magnetic catch and release [12] have been proposed and met with varying degrees of success.

In this paper, we report a novel method for performing MgFFF without invoking irreversible magnetic trapping of the analytes in a spiral separation channel. Our method is based on the use of a rotating magnetic field on top of the separation channel to provide periodically changed force field acting on the particles. When the rotating magnet sweeps over the particles of different sizes, they are all lifted to the top wall region by magnetophoresis. As the rotation of the magnet continues, its influence on the particles is rapidly diminished and the particles begin to relax into different flow streamlines under gravity. Adsorption of the particles at internal channel surface is prevented due to short residence time which is

* Corresponding author. Postal address: Room #A405, Building #24, Tianjin University, 92 Weijin Road, Nankai District, Tianjin 300072, China.
Tel.: +86 22 27403650; fax: +86 22 27403650.
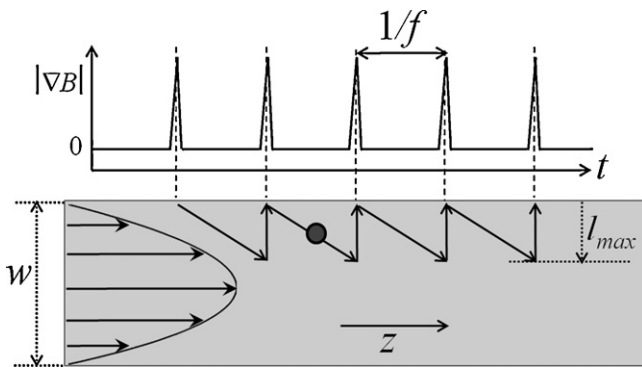E-mail address: qhwan@tju.edu.cn (Q.-H. Wan).

Fig. 1. Time-dependent behavior of magnetic field and particle motion in CyMgFFF with a magnet rotation frequency of f. $l_{\max}$ is the maximum distance the particle travels under gravity in one cycle.

controlled by the rotation frequency. With recycling of such a catch-release process, the particles assume saw-tooth like downstream migration trajectories and travel out of the separation channel at velocities corresponding to their sedimentation coefficients. A retention model taking into account the effects of magnetic, gravitational forces, and hydrodynamic flow was proposed and evaluated with experimental data obtained using 6.04- and 9.40-μm diameter magnetic microspheres. The method described here is advantageous over those previously reported in that separation efficiency and resolution can be greatly improved by tuning the strength and rotation frequency of the magnetic field in addition to flow rate. Unlike Nomizu et al's method [10] where periodical intermittent magnetic field is applied to a separation column but no separation of magnetic particles is possible, the frequency of changing magnetic field in our method is much high so as to induce differential distribution of the particles across the separation channel. Our method also differs from Beveridge et al's method [12] where the catch and release action occurs when a stepped increase and decrease of magnetic field is applied to the separation channel. The strong magnetically responsive species are trapped earlier on the capillary but eluted later than the weak magnetic species, both showing rather tailed peaks.

2. Theory

Cyclic magnetic field-flow fractionation (CyMgFFF) developed in this work is carried out in an open-tubular capillary, which is wound several turns to form a flat spiral coil. A rotary magnet is placed above the capillary coil to provide a cyclic magnetic field across the capillary. A steady stream of an eluent is pumped through the capillary. A mixture of magnetic species such as magnetic particles is introduced as a narrow band that is held at the top wall of the capillary before the magnet is set into rotation to begin separation. As the species move downstream with the flowing fluid, they migrate up and down between the walls of the capillary as they are driven alternately by the opposing magnetic and gravitational field. Heavy species penetrate deep into the parabolic flow, and as a result they acquire higher velocities than the light species during each cycle, if the maximum distance the species migrate transversely is limited not to beyond the central line of the capillary.

Consider a magnetic particle of radius r suspended in a flowing fluid in an open-tubular capillary channel of diameter w is subjected to a rotating magnetic field B applied from above the capillary and normal to the fluid flow direction. The particle experiences an up and down force alternately and thus undergoes a saw-tooth like motion as depicted in Fig. 1. This motion of the magnetic particle induced by such an alternating field can be analyzed in terms of

transverse and longitudinal components with Brownian diffusion neglected for clarity [13,14].

2.1. Transverse migration of magnetic particles

In a non-uniform magnetic field gradient as shown in Fig. 1, the magnetic force F_m acting on a magnetic bead is balanced by the viscous drag force F_d and gravitational force F_g [15,16]:

$$F_m + F_d + F_g = 0 \tag{1}$$

where

$$F_m = V_p M_s \nabla B$$

$$F_d = -6\pi \eta r U$$

$$F_g = V_p(\rho_p - \rho_m)g$$

M_s is the saturation magnetization of the sample, ∇B is the magnetic field gradient, η is the viscosity of fluid, U is the transverse velocity of the particle, ρ_p and ρ_m are the respective densities of the particle and medium, and g is the acceleration due to gravity. Solving for U and observing that $V_p = 4/3\,\pi r^3$, we obtain

$$U = \frac{2r^2[M_s \Delta B + (\rho_p - \rho_m)g]}{9\eta} \tag{2}$$

From Eq. (2), it can be seen that the upward velocity of the particle induced by the magnetic field is directly proportional to the size and the magnetization of the particle, and magnetic field gradient which has a negative sign to reflect the fact that it decreases with the distance between the field and particle. Obviously, when the magnetic field is removed, the magnetic microsphere sediments with a velocity U_{sed} defined by the following equation:

$$U_{sed} = \frac{2r^2(\rho_p - \rho_m)g}{9\eta} \tag{3}$$

The sedimentation coefficient of the particle, s, is then given by

$$s = \frac{U_{sed}}{g} = \frac{2r^2(\rho_p - \rho_m)}{9\eta} \tag{4}$$

Consider a cycle in which the magnetic particles are allowed to relax from the top wall of the capillary. The lateral position of the particle $l(t)$ is a function of time until the bottom wall is reached:

$$l(t) = U_{sed}t \tag{5}$$

The maximum distance $l_{\max}$ the particle travels in one cycle with frequency f is given by

$$l_{\max} = \frac{U_{sed}}{f} \tag{6}$$

A dimensionless retention parameter, λ, is defined as the ratio of the maximum distance a particle travels in the channel $l_{\max}$ to the diameter of the channel w.

$$l = \frac{l_{\max}}{w} = \frac{U_{sed}}{fw} \tag{7}$$

Three operation modes can be defined based on the value of λ [13,14]. In the case of $\lambda < 1$, the system is said to be operating in mode I. In this mode the maximum distance a particle travels from the top wall is always less than the thickness of the channel, w. If λ is larger than 1, the system is said to be operating in mode III. In this case, the particle arrives at the bottom wall before the field cycle ends and thus migrates by the steric mechanism for the remaining time. The system is operating in mode II when λ is equal to 1. The particle travels maximum distance which is equivalent to the channel thickness.

2.2. Longitudinal migration of magnetic particles

A continuous steady stream of carrier fluid flows through the separation channel. A symmetric Poiseuille velocity profile is formed during the flow through the circular capillary tubing [17]:

$$\upsilon(l) = 8\upsilon_o \left(\frac{l}{w} - \frac{l^2}{w^2} \right) \tag{8}$$

where $\upsilon(l)$ is the fluid velocity in the flow direction at the distance l from the top wall of the capillary and υ_o is the average carrier fluid velocity, which is half that of the fluid velocity at the center of the capillary. The longitudinal particle displacement Z in one cycle can be expressed as

$$Z = \int_0^{1/f} \upsilon(l)dt \tag{9}$$

Changing the variable of integration from t to l using Eq. (5), we obtain

$$Z = \int_0^{l_{max}} \frac{\upsilon(l)}{U_{sed}}dl \tag{10}$$

The substitution of Eq. (3) into this expression followed by integration and the use of Eq. (7), we obtain

$$Z = \frac{4\upsilon_o\lambda}{f} \left(1 - \frac{2\lambda}{3} \right) \tag{11}$$

The average longitudinal displacement velocity for the particle υ_p can be written as

$$\upsilon_p = \frac{Z}{1/f} = 4\upsilon_o\lambda \left(1 - \frac{2\lambda}{3} \right) \tag{12}$$

2.3. Retention of magnetic particles

A dimensionless retention ratio R is defined as a ratio of the longitudinal migration velocity of the particle υ_p to that of the carrier fluid υ_o:

$$R = \frac{\upsilon_p}{\upsilon_o} = 4\lambda \left(1 - \frac{2\lambda}{3} \right) \tag{13}$$

when taking into account the finite size of the particle which leads to exclusion of its center of mass from a layer adjacent to each channel wall of thickness r, a modified equation for the retention ratio can be derived [14]:

$$R = 4\lambda \left(1 - \frac{2\lambda}{3} \right) + 8\alpha(1 - \alpha - \lambda) \tag{14}$$

where $\alpha = r/w$.

Since λ is proportional to the particle diameter squared, the rate at which R changes with λ can be taken as a measure of selectivity, S, of the separation system operating in mode I. Thus we define S as $dR/d\lambda$

$$S = \frac{dR}{d\lambda} = 4 - \frac{16}{3}\lambda - 8\alpha \tag{15}$$

S has a maximum value of $4-8\alpha$ at $\lambda = 0$ and then decreases with increasing λ, suggesting that separation is preferably carried out at small values of λ if a high selectivity is desired.

3. Experimental

3.1. Reagents and materials

Monodispersed polystyrene microspheres of diameters 5.3- and 8.6-μm (BaseLine Chromtech Research Centre, Tianjin, China), polyethylenimine (PEI, MW 20000, Qianglong New Materials,
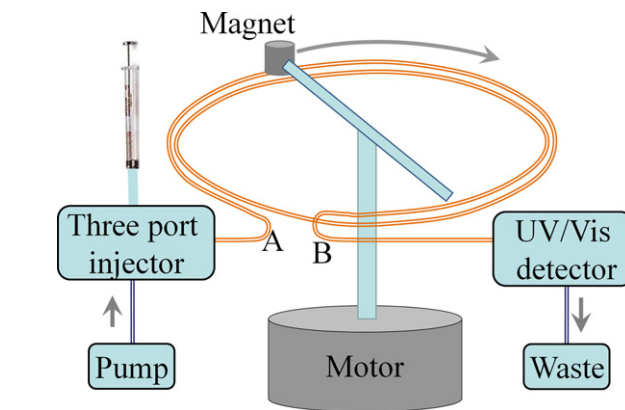

Fig. 2. Schematic diagram showing the field-flow fractionation system with a rotating magnetic field.

Wuhan, China), tetraethoxysilane (TEOS, Wuhan University Silicone New Materials, Wuhan, China) and acetonitrile (HPLC grade, Concord Technology, Tianjin, China) were used as received from the manufacturers. Sodium citrate stabilized magnetite nanoparticles were prepared according to a literature method [18].

3.2. Synthesis and characterization of magnetic microspheres

Core–shell structured magnetic microspheres were synthesized by a layer-by-layer self-assembly method as described in the literature [19,20]. Briefly, 4 g of polystyrene microspheres were dispersed in 100 mL of 2% polyethylenimine (PEI) aqueous solution under sonication. The particles were retrieved by centrifugation at 3000 rpm for 10 min, washed with deionised (DI) water twice and then redispersed in 50 mL DI water. An aqueous magnetite nanoparticle solution (0.5%) was dropwise added into the microsphere suspension with stirring. The negatively charged magnetite nanoparticles were immobilized on the positively charged polystyrene microspheres through electrostatic interactions. The addition of the magnetic colloids was terminated when the color of the suspension turned into brown and the total volume of the magnetite fluid added was about 20 mL. The magnetite-coated microspheres were separated by magnetic decantation and washed twice with DI water. This coating procedure was repeated six times to enhance the magnetic responsivity. Finally, to protect the magnetite embedded in the outer surface from leaching, a thin layer of silica was applied to the core–shell structured magnetic microspheres using a sol–gel method.

The particle size distributions (PSDs) of magnetic particle samples were determined using a Multisizer 3 Coulter Counter (Beckman Coulter, Brea, CA, USA) with a 100 μm aperture tube. The resulting PSD curves (number of particles counted $N(x)$ vs particle diameter x) were treated approximately as Gaussian curves and used to calculate mean particle sizes μ (the x value at which the number of particles is a maximum) and standard deviations σ (σ = FWHM/2.35, where FWHM is the full width at half maximum). The magnetic properties of the particle samples were obtained with a LDJ 9600-1 vibrating sample magnetometer (LDJ Electronic, Troy, MI, USA). The densities of the magnetic microspheres were determined by gravimetric method with a 25-mL pycnometer.

3.3. Cyclical magnetic separation instrumentation

The separation system as shown in Fig. 2 consisted of a Spectroflow 400 HPLC pump (Applied Biosystems, Foster City, CA, USA), a three port injector constructed in house on a PEEK tee-piece adaptor fitted with a needle guide and a 25- or 100-μL microsyringe,

a fused silica capillary (180 cm length, 250 μm inner diameter, 360 μm outer diameter, Xinnuo Chromatography Products, Handan, China), a rotating magnet fixed on a steel tee-piece, a Spectra 100 Variable UV–Visible CE Detector (Thermo Separation Products, San Jose, CA, USA) and a N2000 chromatography data system (BaseLine Chromtech Research Centre, Tianjin, China). The tubular capillary was wound 6.5 turns on a plastic sheet and covered with a sheet of transparent tape, yielding a flat spiral coil with a length of 153 cm and a diameter of 7.5 cm. This flat coil was placed horizontally under the influence of a cyclical magnetic field produced by a 10-mm diameter, 8-mm thick NdFeB rare earth magnetic disk (~0.4 T on the flat surface) undergoing a circular motion in the direction same as with fluid. The rotating magnet was driven by a miniangle stepper motor (M091-FD09, The Superior Electric Company, Bristol, CT, USA) with a speed controller provided by Waters (Waters, Milford, MA, USA). A Model CT3-A gaussmeter (No 4 Electric Instrument Works, Shanghai, China) was used to determine the variation of the magnetic flux produced by the magnet over the distance from its surface.

3.4. Particle separation procedures

The fluid carrier acetonitrile was pumped through the capillary at 0.04 mL/min unless otherwise specified. Prior to sample injection, the magnet was positioned near the inlet end of the flat spiral coil (Fig. 2, point A). The particle suspension (2 mg/mL magnetic microspheres except for sample loading experiments in which the particle suspension of 10 mg/mL was used) was injected through a three port injector and accumulated at point A by magnetic attraction. Elution was continued for 3 min to wash off interfering impurities and then the stepper motor was turned on to set the magnet into rotation and the elution curve was measured at detection wavelength of 400 nm. The retention time is denoted as t_{r1}. When the particles move out of the influence of the magnetic field near the outlet end (Fig. 2, point B), their transport rates are altered. This post-magnetic-field retention time was determined by measuring the time the particles take to migrate from point B to detection cell without the influence of the magnetic field. The retention time is denoted as t_{r2}.

The mean velocity of the fluid, υ_o, was determined by measuring the time a bubble takes to migrate from injection point to the detection cell t_o and calculated according to $\upsilon_o = L_o/t_o$ where L_o is the total length of the capillary.

The retention ratio of the particle, R, is calculated according to the following equation:

$$R = \frac{\upsilon_p}{\upsilon_o} = \frac{L_{eff}}{t_{r1} - t_{r2}} \cdot \frac{t_o}{L_o} \qquad (16)$$

where L_{eff} is the effective length of the capillary covered by the rotating magnet, which is 1.53 m.

4. Results and discussion

4.1. Characterization of magnetic particles

To be used as standard particles for model validation and system evaluation, two types of core–shell structured magnetic microspheres were synthesized and characterized. The particle size distribution curves (Fig. 3A) show that the synthesized particles have mean particle diameters of 6.04 μm and 9.40 μm, respectively, with relative standard deviations less than 5%. The lack of hysteresis in magnetization curves (Fig. 3B) suggests that both of the magnetic particles are superparamagnetic. This property makes them particularly suited as testing materials for the fact that the induced magnetization is lost when the magnetic field is removed so that the formation of particle clusters by magnetic attraction is
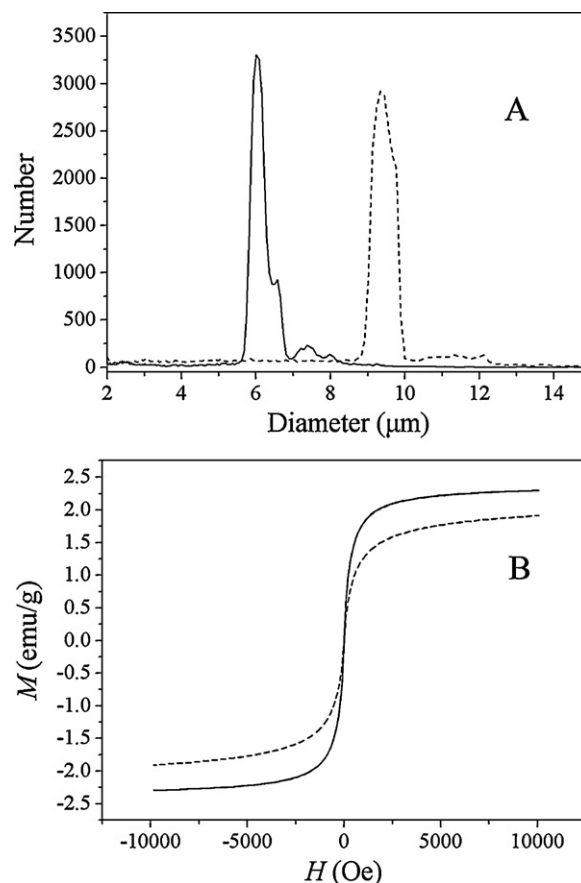

Fig. 3. (A) Particle size distribution curves and (B) magnetization curves of the two types of magnetic microspheres synthesized. Solid and dotted lines correspond to 6.04-μm and 9.40-μm diameter particles, respectively.

reversible. The physical and transport properties of the synthesized magnetic particles are summarized in Table 1.

4.2. Effect of rotation frequency on particle retention

The rotation frequency of the magnetic field is of paramount importance in this mode of separation as it determines the maximum distance a particle migrates transversely and consequently the retention. The retention ratios for two types of magnetic particles were determined as a function of frequency at three different flow rates 0.01, 0.02 and 0.04 mL/min with 10 μg sample loaded. As shown in Fig. 4, the retention ratio increases initially with the frequency until a maximum is reached at 0.33 Hz for 6.04-μm and 0.55 Hz for 9.40-μm particles. The R value decreases slowly afterwards. Similar patterns were observed at all three different flow rates. The frequency-dependent behavior of the particle retention can be described by the theoretical model presented above. Theoretical curves calculated by Eq. (14) were fitted with the experimental data and the results are shown in Fig. 4. In qualitative terms, the retention model gives a reasonable account of the variation of the retention ratio of magnetic particle with the rotation frequency

Table 1
Physical and migration properties of two magnetic microspheres used.

r (μm)	ρ_p (g/cm³)	M_s (emu/g)	U_{sed} (μm/s)[a]	s (μs)[a]
3.02 ± 0.09	1.24	2.30	24.7	2.52
4.70 ± 0.16	1.19	1.91	53.4	5.45

[a] The data for transverse velocity, U_{sed}, and sedimentation coefficient, s, were calculated by Eqs. (3) and (4) using ρ_m = 0.769 g/mL, and η = 0.379 × 10⁻³ Pa s.

Fig. 6. Dependence of retention ratio R of 6.04-μm (■) and 9.40-μm (▲) particles on the distance x from the magnet surface (~400 mT). Magnet rotation frequency, 2.21 Hz; carrier flow rate, 0.04 mL/min; other conditions same as for Fig. 4.

4.3. Effect of the gap between magnet and separation channel on particle retention

The driving force to lift particles toward the top wall of the capillary is magnetic field gradient $\triangledown B$, which decreases with the distance x from the magnet surface. The magnetic force acting on the magnetic particles decreases with the gap between the magnet and the separation channel. With the frequency of the rotating magnet set at 2.21 Hz, the retention ratios for two types of magnetic particles were determined as a function of the distance from the magnet surface. As shown in Fig. 6, the retention ratio of the 6.04-μm particle is essentially unchanged with increasing distance until $x = 2.5$ mm. Afterwards, the R value increases sharply and reaches a maximum at 4.6 mm. The retention decreases rather steadily with further increase in the distance. Similar trend was observed for 9.4-μm particles except that the maximum occurs at shorter distance. The changes observed reflect the influence of the magnetic field strength which decreases rather steeply with an increase in the gap. At short distances, the magnetic field strength is high enough to lift all particles to the top wall of the capillary. Because the particles are held in the near wall regions they migrate through the separation channel with low velocities. With an increase in the distance, the magnetic force acting on the particles is weakened and the particles excurse into the center regions. In this case we observe an increase in the retention ratio. The particles tend to move by steric mechanism [21] with further increase in the distance as a result of diminishing magnetic field. From the data shown in Fig. 6, it appears that the gap between the magnet and separation channel should be kept less than 3 mm to attain optimum retention and separation of magnetic particles.

4.4. Effect of carrier flow rate on particle retention

According to the retention model presented above, the retention ratio of a particle is independent on the carrier flow rate. However, if secondary effects such as hydrodynamic lift force set in, a deviation from linearity would occur. Therefore, an investigation of flow rate effects should provide some useful insights into the mechanism of retention under study. In addition, an increase in flow rate produces a high shear force on the particle and this may have positive impact on peak shape as a result of reduced magnetic particle trapping.

With the rotation frequency of the magnet set at 2.21 Hz and the gap at 0.48 mm, the fractograms for a mixture of 6.04-μm and 9.40-μm magnetic microspheres were recorded at varying carrier flow rates. As shown in Fig. 7, the retention times of the particles

Fig. 4. Retention ratio R as a function of magnet rotation frequency f for (A) 6.04-μm and (B) 9.40-μm beads at three different flow rates 0.01 (■), 0.02 (●) and 0.04 (▲) mL/min under model I conditions. Magnetic induction on the surface of the magnet, ~400 mT; the gap between magnet and capillary, 0.48 mm; carrier fluid, acetonitrile; detection, 400 nm; sample loading, 10 μg. The theoretical curves are plotted by Eq. (14).

of magnetic field. In quantitative terms, however, the experimental results deviate substantially from those predicted by theory, especially in low frequency regions. The theoretical values for maximum R occur at frequencies lower than those for experimental data, suggesting that there is an increase in the settling velocity measured as compared with that calculated from Stokes equation. The shift of frequency due to increased sedimentation is illustrated in Fig. 5. Particles of two different sedimentation coefficients start to migrate at the same time but reach the central line of the capillary at different frequencies. The light particle arrives at the central line and thus assumes the maximum velocity at frequency lower than that for heavy one. It is likely that the sedimentation coefficient in the Stocks equation is underestimated due to concentration, viscosity, and hydrodynamic effects [14].
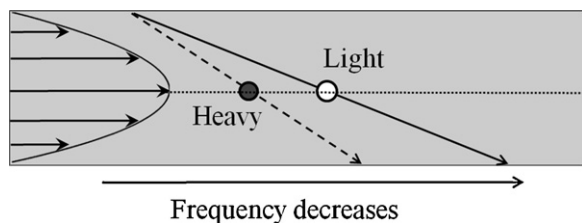

Fig. 5. Heavy (solid) and light (hollow) particles arrive at central line at different frequencies.
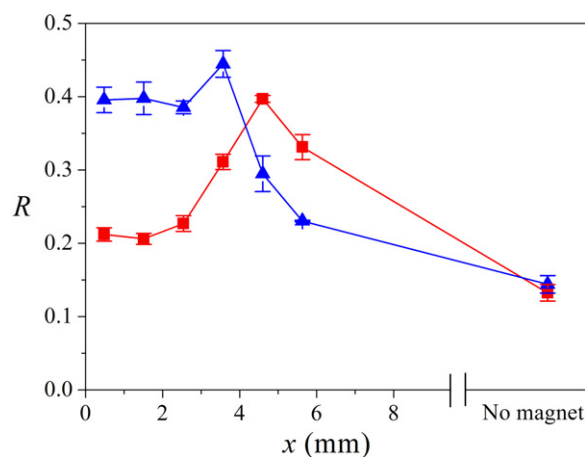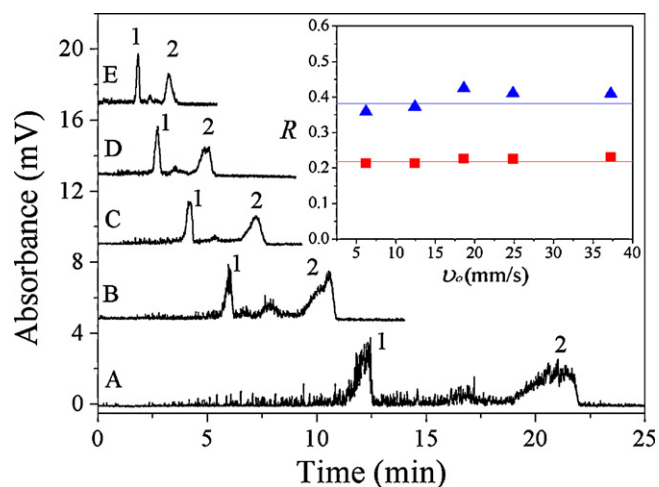
Fig. 7. Separation of magnetic microspheres obtained at varying flow rate: (A) 0.02 mL/min; (B) 0.04 mL/min; (C) 0.06 mL/min; (D) 0.08 mL/min; and (E) 0.12 mL/min. Magnet rotation frequency, 2.21 Hz; other conditions same as for Fig. 4. Peak identification: 1, 9.40-μm diameter particles; 2, 6.04-μm diameter particles. Average retention ratios of 0.222 and 0.395 were calculated from data shown in inset for 6.04-μm ($\blacksquare$) and 9.40-μm ($\blacktriangle$) particles, respectively.

decrease with increasing carrier flow rate but the retention ratios remain unchanged (Fig. 7, inset). The constant retention ratios for the particles tested exclude the possible interference of hydrodynamic lift force with the separation under the conditions employed. A tendency is noticeable from the fractograms that peak shape is steadily improved with increasing flow rate. These observations confirm that optimum separation of magnetic particles with increased efficiency can be achieved by tuning the magnetic field gradient, rotation frequency and carrier flow rate.

4.5. Effect of sample loading on particle retention

To test the linear range of the sample loading in this mode of separation, varying volumes of a particle suspension (10 mg/mL) were injected. The retention ratios as a function of sample loading are shown in Fig. 8. In the range 10–200 μg of particle sample, the retention ratio increases slightly, with variations less than 25%. In the range 200–750 μg, the increases in retention ratio become more prominent with variations mounting to 100%. Two different mechanisms were invoked to account for the rather narrow linearity observed. At low sample loadings, space dispersion of
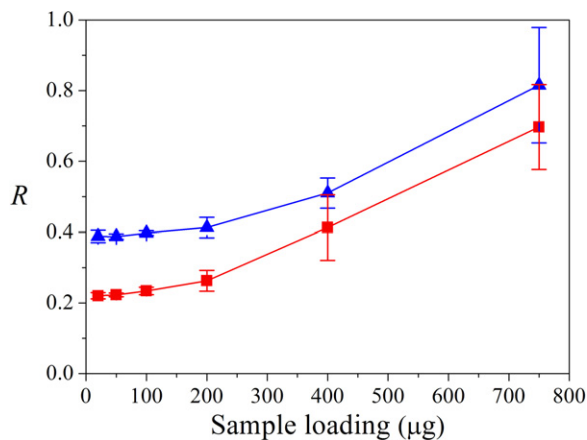
the particle is probably responsible for slight decrease in retention time. This means that when the magnetic field sweeps off, not all the particles are set into motion from the same starting point. The particles located further away from the walls would assume the greater migration velocity and thus greater retention ratio. The greater variation in retention ratio observed for high sample loading is associated with the limited surface area available for particle immobilization. With increasing sample loading, the surface area covered by the size of the magnet tends to be saturated. When the amount of particles loaded exceeds its loading capacity, particle leakage into the flow fluid occurs, leading to a significant increase in the retention ratio.

5. Conclusions

To tackle particle entrapment problem frequently encountered in magnetic field-flow fractionation (MgFFF), we have developed a new approach mimicking the reversible magnetic catch and release action. Our approach is based on the use of a rotating magnetic field to generate a periodically changing gravitational field acting on the particles. Under the action of such a cyclical field, magnetic particles transported by a laminar flow have retention behavior primarily determined by their transport properties. This separation technique represents an important and fundamentally new advance in the field of FFF, as it is demonstrated for the first time that high efficiency separation of magnetic particles can be achieved by tuning the frequency of a rotating magnetic field in addition to magnetic field gradient and carrier flow rate.

Current demonstration of the technique has been limited to the separation of micrometer-sized, unfunctionalized magnetic microspheres, however, cyclical MgFFF can also be applied to biological/biomedical analysis as long as magnetic labeling technique and/or formation of magnetic clusters are involved [3]. Particularly, the technique can be used as the size-based separation method to sort out various magnetic microspheres coated with different antibodies as well as to distinguish between dimers, trimers, and other magnetic bead-protein/cell complexes [22]. Although size separation of magnetic particles can also be achieved by other FFF techniques, MgFFF offers a distinct advantage in that non-magnetic particles such as unlabeled species can be flushed away after injection so that their potential interference with the separation is removed even before the separation is started. As such, cyclical MgFFF holds promise for a number of bioanalytical applications where it can be applied to isolation and identification of multiple analytes with an efficiency that is difficult to accomplish by alternate separation techniques [23].

Fig. 8. Variation of retention ratio of the 6.04-μm ($\blacksquare$) and 9.40-μm ($\blacktriangle$) particles with sample loading. Magnet rotation frequency, 2.21 Hz; carrier flow rate, 0.04 mL/min; other conditions same as for Fig. 4.

References

[1] J.C. Giddings, Science 260 (1993) 1456.
[2] M. Schimpf, K. Caldwell, JC. Giddings (Eds.), Field-flow Fractionation Handbook, John Wiley & Sons, New York, 2000.
[3] P. Reschiglian, A. Zattoni, B. Roda, E. Michelini, A. Roda, Trends Biotechnol. 23 (2005) 475.
[4] R.C. Willis, Today's Chemist at Work, 2002, p. 21.
[5] S.K.R. Williams, J.R. Runyon, A.A. Ashames, Anal. Chem. 83 (2011) 634.
[6] T.M. Vickrey, J.A. Garcia-Ramirez, Sep. Sci. Technol. 15 (1980) 1297.
[7] P.S. Williams, F. Carpino, M. Zborowski, Mol. Pharmacol. 6 (2009) 1290.
[8] P.S. Williams, F. Carpino, M. Zborowski, Phil. Trans. R. Soc. A 368 (2010) 4419.
[9] T. Nomizu, H. Nakashima, M. Sato, T. Tanaka, H. Kawaguchi, Anal. Sci. 12 (1996) 829.
[10] T. Nomizu, K. Yamamoto, M. Watanabe, Anal. Sci. 17 (Supplement) (2001) i177.
[11] A.H. Latham, R.S. Freitas, P. Schiffer, M.E. Williams, Anal. Chem. 77 (2005) 5055.

[12] J.S. Beveridge, J.R. Stephens, A.H. Latham, M.E. Williams, Anal. Chem. 81 (2009) 9618.

[13] J.C. Giddings, Anal. Chem. 58 (1986) 2052.

[14] S. Lee, M.N. Myers, R. Beckett, J.C. Giddings, Anal. Chem. 60 (1988) 1129.

[15] M. Zborowski, in: U. Hafeli, W. Schutt, J. Teller, M. Zborowski (Eds.), Scientific and Clinical Applications of Magnetic Carriers, Plenum Press, New York, 1997, pp. 205.

[16] C.T. Yavuz, J.T. Mayo, W.W. Yu, A. Prakash, J.C. Falkner, S. Yean, L.L. Cong, H.J. Shipley, A. Kan, M. Tomson, D. Natelson, V.L. Colvin, Science 314 (2006) 964.

[17] F.M. White, Viscous Fluid Flow, 3rd ed., McGraw-Hill, Columbus, 2006.

[18] Y.H. Deng, W.L. Yang, C.C. Wang, S.K. Fu, Adv. Mater. 15 (2003) 1729.

[19] L. Zhang, L. Chen, Q.-H. Wan, Chem. Mater. 20 (2008) 3345.

[20] F. Chen, R.B. Shi, Y. Xue, L. Chen, Q.-H. Wan, J. Magn. Magn. Mater. 322 (2010) 2439.

[21] T. Koch, J.C. Giddings, Anal. Chem. 58 (1986) 994.

[22] P. Reschiglian, A. Zattoni, D. Melucci, B. Roda, M. Guardigli, A. Roda, J. Sep. Sci. 26 (2003) 1417.

[23] J. Li, J. Ge, Y. Yin, W. Zhong, Anal. Chem. 80 (2008) 7068.